

Electron-paramagnetic-resonance identification of silver centers in silicon

N. T. Son,* V. E. Kustov,[†] T. Gregorkiewicz, and C. A. J. Ammerlaan

*Van der Waals-Zeeman Laboratorium der Universiteit van Amsterdam,
Valckenierstraat 65, NL-1018 XE Amsterdam, The Netherlands*

(Received 18 February 1992)

The observation of silver in silicon by electron paramagnetic resonance (EPR) is reported. In *p*-type silicon doped with silver, several EPR spectra were detected. Three of these, which are labeled Si-NL42, Si-NL43, and Si-NL44, exhibit hyperfine structure with splitting into two components of equal intensity. The spectrum Si-NL42 with the isotropic Zeeman splitting factor $g = 1.9744$ and an isotropic twofold hyperfine splitting was observed in samples doped with natural silver, as well as in samples doped with silver enriched with one of its isotopes ^{107}Ag and ^{109}Ag . The features of the spectrum allow its identification with an isolated interstitial silver atom. The spectra Si-NL43 and Si-NL44 have trigonal symmetry and can be described by an effective electron spin $S = \frac{1}{2}$ and one nuclear spin $I = \frac{1}{2}$. With the perpendicular g value nearly 4, the Si-NL44 spectrum can be better analyzed using electron spin $S = \frac{3}{2}$. By observing an additional twofold splitting in a sample co-doped with ^{57}Fe isotope ($I = \frac{1}{2}$), the spectrum Si-NL43 is shown to arise from an FeAg pair. From the magnitude of the hyperfine splitting as observed in the samples doped with silver enriched with ^{107}Ag or ^{109}Ag isotopes, all centers are confirmed to be silver related.

I. INTRODUCTION

Like other noble metals, silver is an important impurity in silicon. Reported data on the maximum solubility range from 10^{16} to 5×10^{17} atoms per cm^3 .¹⁻³ The electrical properties of silver in silicon have been extensively studied and a number of investigations of Ag-related deep levels in silicon have been reported.⁴⁻¹⁰ Although, again, there exists some scatter in the data, all these investigations seem to indicate that silver introduces two deep levels in silicon: a donor level in the lower half of the band gap and an acceptor level near the middle of the gap. In a recent study based on combined results from thermal and optical measurements, using the deep-level-transient-spectroscopy technique, Baber *et al.*¹¹ have reported that silver creates an acceptor level at $E_c - 0.54$ eV and a donor level at $E_v + 0.34$ eV. These deep levels are in close vicinity of the acceptor and donor levels of gold in silicon. This is not surprising, since the electronic configuration of the free silver atom is similar to that of gold, and also to copper. Consequently, due to the resemblance of this configuration to Au^0 , and to Pt^- as well, it is reasonable to expect that isolated substitutional silver is paramagnetic. Theoretical calculations of the electronic structure of Cu, Ag, and Au, which were carried out by Fazzio, Caldas, and Zunger,¹² have also supported such an assumption. No electron paramagnetic resonance (EPR) spectrum confirming the existence of the paramagnetic state for either of these isolated impurities has been obtained, to the authors' knowledge.¹³ Nevertheless, a number of papers has been published revealing several gold- and copper-related defect complexes. For the silver dopant no EPR investigation has been reported so far, to our knowledge.

In this paper, the EPR observation of silver in silicon is reported. Among several EPR spectra that were found in

silver-doped silicon, three centers have a well-resolved hyperfine structure related to a nuclear spin $I = \frac{1}{2}$. The spectra, labeled Si-NL42, Si-NL43, and Si-NL44, are presented in the paper. Section III gives detailed information on the analysis of these spectra and proposals for microscopic models for the relevant centers.

II. EXPERIMENTAL DETAILS

In order to prepare samples for the study, silver was diffused into commercially available high-grade silicon. In view of the expected location of deep silver-related levels in the band gap of silicon, high-resistivity *n*- and *p*-type materials were chosen. For the studies described in this paper, float-zone, dislocation-free, *p*-type, boron-doped silicon with a resistivity of approximately 1000 $\Omega \text{ cm}$ at room temperature was used as a starting material. Typical dimensions of the samples were $1.5 \times 1.5 \times 15 \text{ mm}^3$ with the longest axis along the crystallographic $[0\bar{1}1]$ direction. Several diffusions were performed with high-purity natural silver containing two isotopes with nearly equal abundance, or with monoisotopically enriched ^{107}Ag (99.5%) or ^{109}Ag (99.4%). For the identification measurement of the FeAg pair, an ^{57}Fe iron isotope enriched to 95.1% was used. Silver and iron diffusion processes were conducted at a temperature of 1250 °C in a closed quartz ampoule filled with 200 mbar of argon. The diffusion times range from 24–40 h, depending on the isotope. After the diffusion process, the samples were quenched in water to room temperature and stored in liquid nitrogen.

The EPR measurements were performed on *X*-band (microwave frequency $\nu \approx 9 \text{ GHz}$) and *K*-band ($\nu \approx 23 \text{ GHz}$) superheterodyne spectrometers. The dispersion part of the magnetic susceptibility was followed with the microwave power kept at the microwatt level. The sam-

ple was mounted with the $[0\bar{1}1]$ direction perpendicular to the plane in which the magnetic field could be rotated. The EPR spectra were measured at liquid-helium temperature.

III. RESULTS AND ANALYSIS

A. Si-NL42 center

The most important result of this study is the observation of an isotropic spectrum that exhibited a hyperfine structure with twofold splitting as illustrated in Fig. 1(a). The spectrum was first observed in a rapidly quenched ^{107}Ag silver-isotope-doped sample. Both spectral components have equal intensity and behave identically with conditions of observation, such as temperature and phase with respect to modulation. The structure of the spectrum is thus understood as being due to the hyperfine interaction with one nuclear spin $I = \frac{1}{2}$ with an abundance of 100%. For the identification of the responsible impur-

ity, one may note that there exist only a few elements with such isotopic composition; these are ^1H , ^{19}F , ^{31}P , ^{89}Y , ^{103}Rh , and ^{169}Tm . However, in view of the doping treatment with a monoisotopic impurity, silver is the obvious candidate for the interpretation of the Si-NL42 spectrum. As the intensity of the Si-NL42 spectrum was rather low, it was not possible to identify the origin of the hyperfine splitting in an electron-nuclear double resonance (ENDOR) experiment. Therefore, to obtain confirmation of the presence of silver in the center, a sample that was similar but doped with the heavier ^{109}Ag isotope was prepared. As depicted in Fig. 1(b), in this sample the Si-NL42 spectrum could also be observed. Comparison of the results obtained for ^{107}Ag and ^{109}Ag , as shown in the Figs. 1(a) and 1(b), respectively, shows a small but distinct difference in the hyperfine splitting. This is very naturally related to the small difference between the nuclear magnetic moments of the two silver isotopes, namely, $\mu = -0.1135\mu_N$ for ^{107}Ag and $\mu = -0.1305\mu_N$ for ^{109}Ag .¹⁴ Indeed, the ratio of the hyperfine splittings as observed in the experiment, equal to 0.87, is in exact agreement with the ratio of the two nuclear magnetic moments. Measurements on these samples were performed in both the X- and K-band spectrometers. An excellent fit of the angular independent experimental data to the spin Hamiltonian

$$H = g\mu_B \mathbf{B} \cdot \mathbf{S} + A \mathbf{S} \cdot \mathbf{I} \quad (1)$$

was obtained with spin $S = \frac{1}{2}$, and Zeeman splitting constant $g = 1.9744$. The full set of parameters as determined for the Si-NL42 spectrum is given in Table I. The significant deviation of the obtained g value from those of other cubic centers in silicon provides additional solid evidence that the Si-NL42 spectrum arises from a different center.

Silver belongs to group IB of the Periodic Table and, as a free atom, has the $4d^{10}5s$ electronic configuration. In the silicon lattice the neutral interstitial silver Ag_i^0 may have the same configuration as the free atom, consistent with the observation of an isotropic spin $S = \frac{1}{2}$ paramagnetic center. However, in the free ^{107}Ag atom the $5s$ electron contact density leads to a hyperfine interaction constant $A = -1831 \text{ MHz}$.¹⁵ The very much reduced value observed for the center in silicon, $A = 4.76 \text{ MHz}$, indicates strong delocalization of the electron. Such an electronic structure is similar to that of shallow donor states. Apparently, these characteristics of the center deviate from those reported for the substitutional silver and suggest the present center to be of interstitial type. The fact that the spectrum could only be observed following fast quenching supports this interpretation. From the intensity of the Si-NL42 spectrum the concentration of the corresponding center is estimated as 10^{13} cm^{-3} . Comparison with the solubility data indicates that the Si-NL42 center represents a small fraction of the total amount of silver present.

Following these arguments, the spectrum Si-NL42 is identified with a neutral isolated silver atom on a high-symmetry interstitial site. Whereas the evidence for the presence of one silver atom on a site of cubic symmetry is

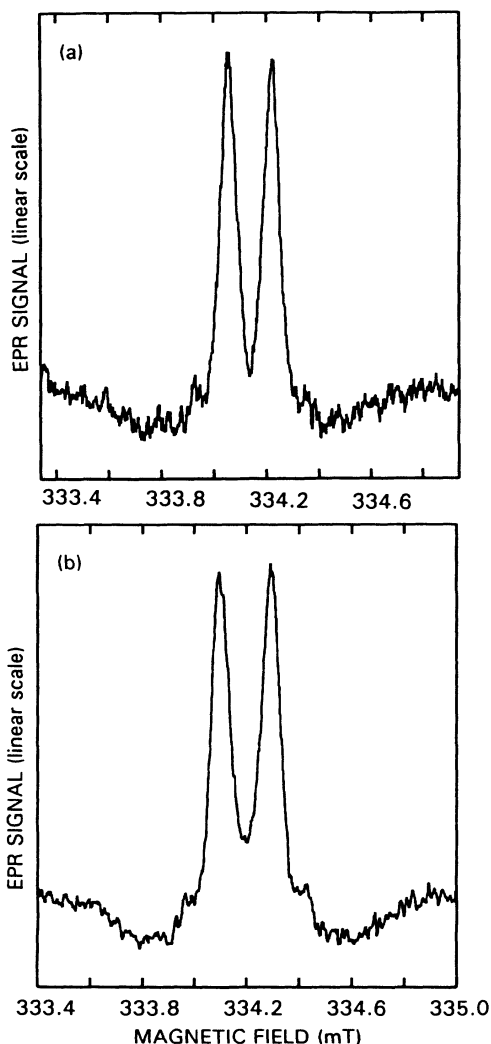


FIG. 1. The isotropic EPR spectrum Si-NL42 as observed for a sample doped with (a) ^{107}Ag (microwave frequency $\nu = 9.2238 \text{ GHz}$) and (b) ^{109}Ag ($\nu = 9.2251 \text{ GHz}$) silver isotopes.

TABLE I. Spin-Hamiltonian parameters of the Si-NL42, Si-NL43, and Si-NL44 centers.

Spectrum	Si-NL42		Si-NL43			Si-NL44	
Spin S	$\frac{1}{2}$		$\frac{1}{2}$			$\frac{1}{2}$	
Isotope	^{107}Ag	^{109}Ag	^{107}Ag	^{109}Ag	^{57}Fe	^{107}Ag	^{109}Ag
g_{\parallel}	1.9744		2.0680			2.0028	
g_{\perp}	1.9744		2.0986			3.9846	
A_{\parallel} (MHz)	4.76	5.47	42.44	48.47	≈ 25	9.0	10.5
A_{\perp} (MHz)	4.76	5.47	29.41	33.12	≈ 19	3.9	4.5
D (GHz)							86

unambiguous, the identification as a single isolated interstitial impurity is based on more indirect interpretation.

B. Si-NL43 center

The Si-NL43 spectrum was observed in silver-doped, p -type silicon, following slower sample quenching. It appeared simultaneously with the Ag-related Si-NL44 center, which will be discussed in Sec. III C. In addition, the well-known spectra of Fe_i^0 , Fe_i^+ , and Ti_i^+ , with which the sample was apparently contaminated during the diffusion process, were present. The Si-NL43 spectrum shows hyperfine structure with the resonance line being split into two components of equal intensity. The trigonal symmetry of the center is evident from its angular dependence, as given in Fig. 2. The intensity of the resonance lines varies considerably with the angle, especially for the higher magnetic-field values, and attains a minimum for the [111] direction. The twofold splitting of the spectrum is indicative of the hyperfine interaction with one 100% abundant nucleus with spin $I = \frac{1}{2}$. In the natural silver, which was used for the preparation of this particular sample, two isotopes, both with nuclear spin value $I = \frac{1}{2}$, were present: ^{107}Ag with an abundance of 51.35% and ^{109}Ag for 48.65%. However, due to a very small difference between the two nuclear magnetic moments of only about 13%, the resonance lines related to different isotopes are nearly coincident. For this reason, not only no splitting but not even a slight asymmetry of the line shape could be detected. Since, similarly to the case of Si-NL42, the intensity of the spectrum did not permit ENDOR measurement, monoisotopically enriched ^{107}Ag and ^{109}Ag isotopes were used to prove the presence of silver in the center. Following the diffusion, basically the same spectrum was observed in samples doped with any of these isotopes, with the linewidth being in both cases narrower than for material doped with the natural silver. Figures 3(a) and 3(b) show EPR spectra as obtained in the [011] direction of the magnetic field for the samples doped with ^{107}Ag and ^{109}Ag silver isotopes, respectively. The apparent difference of the hyperfine splitting may be noticed. The ratios of the hyperfine values as measured at low- and high-field points in the [011] direction are 0.89 and 0.88, respectively. Again, this is in good agreement with the value 0.87 of the ratio of nuclear magnetic moments of the two isotopes. Similarly as for Si-NL42, the result depicted in

Fig. 3 provides direct evidence for the participation of one silver atom in the Si-NL43 center. Rather than by inspection of Fig. 3, the same conclusion is reached by comparing the principal values of the hyperfine interaction tensors, which were determined for the two isotopes from the computer fits of the experimental data (see Table I).

In view of the trigonal symmetry and $S = \frac{1}{2}$ spin value on one side and the electronic configuration of silver on the other, it was difficult to imagine that the center would

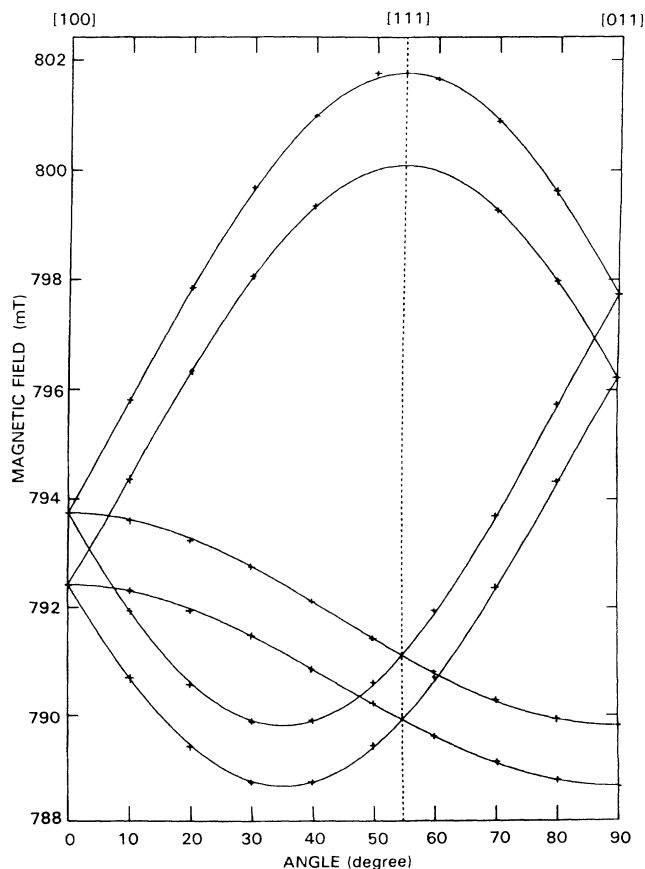


FIG. 2. Angular dependence of the EPR spectrum Si-NL43. The magnetic field is rotated in the (011) plane. The solid curves represent a fit to the experimental points of the ^{109}Ag hyperfine lines according to Eq. (2). The microwave frequency is $\nu = 23.182$ GHz.

consist of a single silver atom only. An impurity pair appeared more likely and, consequently, a second component was searched for. In a sample co-doped with enriched ^{57}Fe , which has nuclear spin $I = \frac{1}{2}$, and ^{109}Ag , an additional splitting of each line was observed, as shown in Fig. 4. The central component of a resonance line in Fig. 4(b) is due to ^{56}Fe with nuclear spin $I=0$ and the two side lines correspond to the hyperfine interaction with one ^{57}Fe isotope. The Si-NL43 spectrum is thus identified as an FeAg pair. A good fit to the experimental data was obtained by using the spin Hamiltonian

$$H = \mu_B \mathbf{B} \cdot \vec{g} \cdot \mathbf{S} + \mathbf{S} \cdot \vec{A}_{\text{Ag}} \cdot \mathbf{I}_{\text{Ag}} + \mathbf{S} \cdot \vec{A}_{\text{Fe}} \cdot \mathbf{I}_{\text{Fe}}, \quad (2)$$

with an electron spin $S = \frac{1}{2}$, nuclear spins $I_{\text{Ag}} = I_{\text{Fe}} = \frac{1}{2}$, and coupling tensors of trigonal symmetry. The full set of parameters as deduced from the fit is given in Table I.

Following the one-electron linear-combination-of-

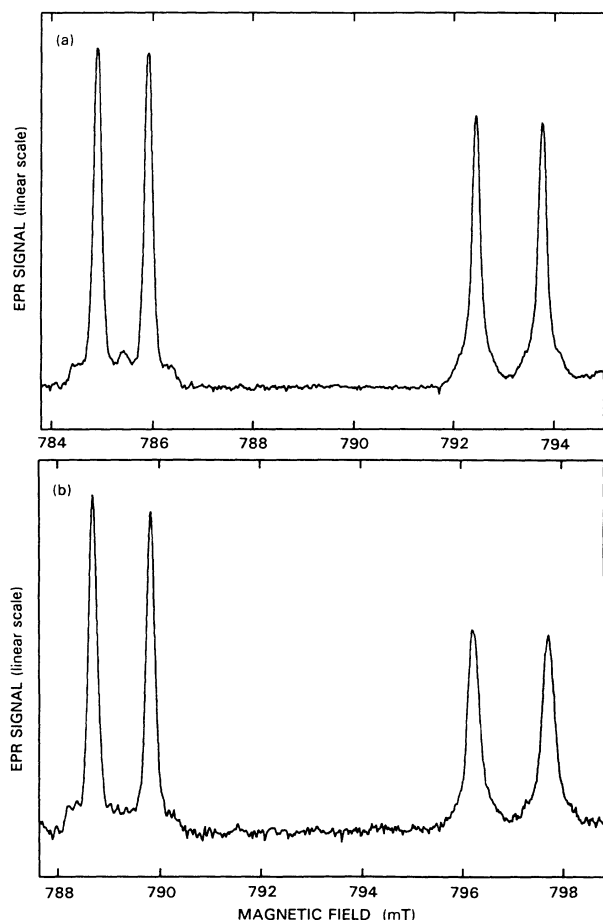


FIG. 3. EPR spectrum of the Si-NL43 center for magnetic field $\mathbf{B} \parallel [011]$ showing the hyperfine structure due to silver nuclei with nuclear spin $I = \frac{1}{2}$ and the difference between ^{107}Ag and ^{109}Ag hyperfine splittings: (a) ^{107}Ag hyperfine structure measured at microwave frequency $\nu = 23.073$ GHz; (b) ^{109}Ag hyperfine structure measured at $\nu = 23.182$ GHz. The scale of the magnetic field is the same in both parts of the figure.

atomic-orbitals (LCAO) approximation, which is known to be suitable for a description of transition-metal impurities in silicon, the wave function of the unpaired electron can be written as a superposition of the electronic wave function of s and d orbitals

$$\Psi = \eta(\alpha\psi_s + \gamma\psi_d). \quad (3)$$

This wave function gives rise to a hyperfine interaction with isotropic and anisotropic components, which can be related to the unpaired spin in the s and d orbitals, respectively. The decomposition of the hyperfine tensor into isotropic and anisotropic parts can be written as

$$\vec{A} = a\vec{1} + \vec{B}. \quad (4)$$

The trace a of tensor \vec{A} , the Fermi contact interaction

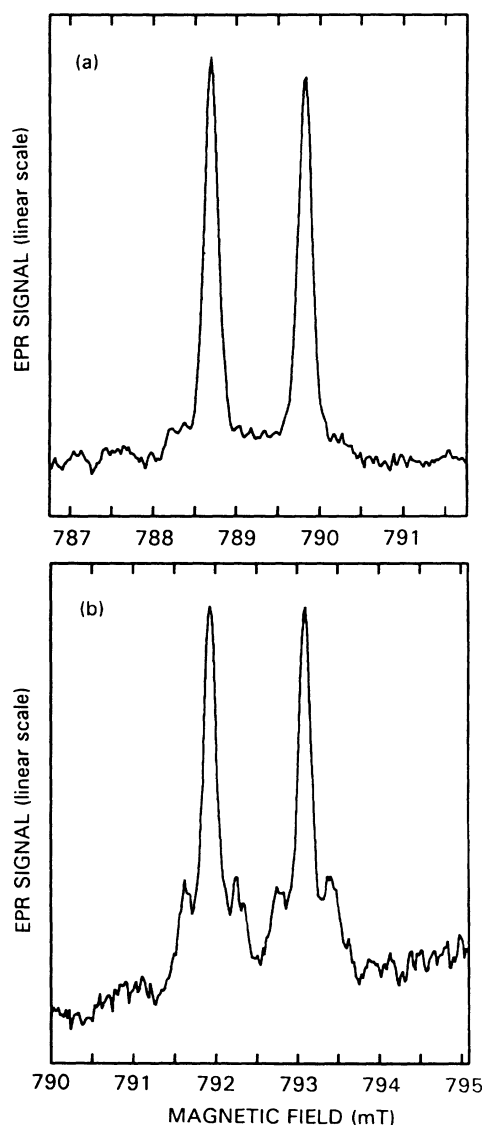


FIG. 4. Part of the EPR spectrum of the Si-NL43 center near the region $g=2.0986$ for $\mathbf{B} \parallel [011]$: (a) the ^{109}Ag hyperfine structure (microwave frequency $\nu = 23.182$ GHz); (b) the additional splitting due to the ^{57}Fe isotope with nuclear spin $I = \frac{1}{2}$; the central component arises from the ^{56}Fe isotope with spin $I=0$ (microwave frequency $\nu = 23.277$ GHz).

term, is given by the spin density $\eta\alpha$ in the s orbital, by the expression

$$a = \frac{1}{3}(A_{\parallel} + 2A_{\perp}) = \frac{2}{3}\mu_0 g \mu_B g_N \mu_N \eta^2 \alpha^2 |\psi_s(0)|^2. \quad (5)$$

The traceless anisotropic part \vec{B} is an axial tensor with principal values $(2b, -b, -b)$, where

$$b = \frac{1}{3}(A_{\parallel} - A_{\perp}) = \left[\frac{1}{4\pi} \right] \mu_0 g \mu_B g_N \mu_N \eta^2 \gamma^2 (\pm \frac{2}{7}) \langle r^{-3} \rangle_d. \quad (6)$$

Using atomic constants given by Morton and Preston,¹⁵ g_N values as tabulated by Fuller,¹⁴ and hyperfine parameters from Table I, the spin densities $\eta^2 \alpha^2$ and $\eta^2 \gamma^2$ in the $5s$ and $4d$ orbitals on the silver atom are found to be 1.8% and 7.4%, respectively. This localization is substantially higher than that found for the Si-NL42 center and suggests a different lattice site for silver in the FeAg pair defect. For iron the spin densities in the $4s$ and $3d$ orbitals are determined to be 2.8% and 7.2%. Parameters from the LCAO analysis of the hyperfine interaction are summarized in Table II.

Due to its high diffusivity, iron is known to form pairs and complexes with other impurities. A number of shallow acceptor-iron and transition impurity-iron pairs in silicon have already been studied in the early 1960s by Ludwig and Woodbury.¹⁶ For the description of impurity-iron pairs in silicon, they proposed a highly successful model that could in all cases account for the observed electron spin values. It is therefore justified to apply their model also to the case of FeAg pairs. The neutral interstitial iron Fe_i^0 has $3d^8$ configuration and an electron spin $S_{\text{Fe}} = 1$. For silver no data revealing its favored lattice position is available. However, from the similarity in electrical properties to gold, it is reasonable to assume that silver will occupy the substitutional position in silicon. In the neutral charge state, the substitutional silver Ag_s^0 has $4d^7 5s 6p^3$ configuration; three missing electrons in the $4d$ shell will result in an orbital singlet state with $S_{\text{Ag}} = \frac{3}{2}$. An antiparallel coupling between iron and silver spins then gives rise to a total spin $S = \frac{1}{2}$, in agreement with the experimental finding. The same total spin can also be obtained for the case of $\text{Fe}_i^+ \text{Ag}_s^-$,

by the antiparallel coupling of spin $S_{\text{Fe}} = \frac{3}{2}$ on Fe_i^+ and spin $S_{\text{Ag}} = 1$ on Ag_s^- . The hyperfine interactions for both the $\text{Fe}_i^0 \text{Ag}_s^0$ and $\text{Fe}_i^+ \text{Ag}_s^-$ models are considered here. The hyperfine interaction, as calculated on the basis of the observed experimental data using total spin $S = \frac{1}{2}$, results in fact from the interactions of the individual electron spins S_{Fe} and S_{Ag} with the individual nuclear spins I_{Fe} and I_{Ag} . The relations between the actual hyperfine parameters A_{Fe} , A_{Ag} and the experimental values $A_{\text{Fe}}^{\text{eff}}$, $A_{\text{Ag}}^{\text{eff}}$ are given by $A_{\text{Fe}} = -(\frac{3}{2})A_{\text{Fe}}^{\text{eff}}$ and $A_{\text{Ag}} = (\frac{3}{2})A_{\text{Ag}}^{\text{eff}}$ for $\text{Fe}_i^0 \text{Ag}_s^0$ and by $A_{\text{Fe}} = (\frac{3}{2})A_{\text{Fe}}^{\text{eff}}$ and $A_{\text{Ag}} = -(\frac{3}{2})A_{\text{Ag}}^{\text{eff}}$ for $\text{Fe}_i^+ \text{Ag}_s^-$ (for a detailed treatment, see Ref. 17). For both cases Eqs. (5) and (6) can still be used with the quantities $\eta^2 \alpha^2 |\psi_s(0)|^2$ and $\eta^2 \gamma^2 \langle r^{-3} \rangle_d$ being replaced by effective wave-function parameters $|\psi_s(0)|_{\text{eff}}^2$ and $\langle r^{-3} \rangle_d^{\text{eff}}$. These effective parameters, as determined from the numerical analysis, are given in Table II. Since the signs of the hyperfine constants are not determined in the experiment, these are ignored. It can be concluded that the values of the effective atomic constants are in all cases much smaller than those found or extrapolated from Hartree-Fock calculations.^{18,19} On the basis of these values, it is difficult to assess which of the two models is more appropriate. However, in view of the similarities of the recent findings to the case of the FeAu pair,^{17,20} for which the electronic $\text{Fe}_i^+ \text{Au}_s^-$ model was adopted, the $\text{Fe}_i^+ \text{Ag}_s^-$ model appears more probable. Interstitial iron has a donor level at $E_v + 0.4$ eV, while a substitutional silver atom may behave either as a donor, with its ionization level at $E_v + 0.34$ eV, i.e., slightly below the iron level, or as an acceptor, with the appropriate level at $E_c - 0.54$ eV, i.e., slightly above the iron level. In this situation, transfer of one electron from iron to silver is conceivable, thus giving rise to Coulomb interaction between two impurities and forming the $\text{Fe}_i^+ \text{Ag}_s^-$ center.

C. Si-NL44 center

As mentioned in Sec. III B, following silver diffusion into p -type silicon another trigonal spectrum, labeled Si-

TABLE II. Hyperfine data from the analysis with different models of the Si:FeAg center (spectrum Si-NL43). The signs of hyperfine constants, which are not determined in the experiment, are taken positive.

Model	a (MHz)	b (MHz)	$\eta^2 \alpha^2$	$\eta^2 \gamma^2$	$ \psi_s(0) _{\text{eff}}^2$ (\AA^{-3})	$\langle r^{-3} \rangle_d^{\text{eff}}$ (\AA^{-3})
LCAO						
$\text{FeAg} = \frac{1}{2}$						
^{109}Ag	38.24	5.12	0.018	0.074	0.89	4.85
^{57}Fe	21	2	0.028	0.072	0.92	2.73
$\text{Fe}_i^0 \text{Ag}_s^0$						
$S_{\text{Ag}} = \frac{3}{2}$						
^{109}Ag	22.94	3.07			0.54	2.90
$S_{\text{Fe}} = 1$						
^{57}Fe	31.5	3.0			1.37	4.10
$\text{Fe}_i^+ \text{Ag}_s^-$						
$S_{\text{Ag}} = 1$						
^{109}Ag	57.34	7.68			1.34	7.28
$S_{\text{Fe}} = \frac{3}{2}$						
^{57}Fe	12.6	1.2			0.55	1.64

NL44, could be observed in addition to the FeAg pair. The angular dependence of the Si-NL43 spectrum as measured in the (011) plane is depicted in Fig. 5. Due to the large anisotropy and a small misorientation of the sample, all four $\langle 111 \rangle$ orientations of the trigonal center are separately visible. The spectrum exhibits some hyperfine structure which, in the natural silver-doped sample, is rather anisotropic and not very well resolved. The line intensity of the Si-NL44 spectrum is much smaller than that of the FeAg pair, reflecting lower concentration of the relevant centers. Similarly as in the case of the FeAg pair, doping with single ^{107}Ag and ^{109}Ag isotopes was used for further identification of the spectrum. In the single-isotope-doped samples, the linewidth was narrower and the hyperfine structure could be resolved better. In Figs. 6(a) and 6(b) the hyperfine structure of the resonance line is shown as observed for ^{107}Ag and ^{109}Ag isotope-doped samples, respectively. As can be concluded from these figures, the difference in the hyperfine splittings reflects exactly the difference of the nuclear moments of the two isotopes, proving the presence of silver in the center.

The angular dependence of the Si-NL44 spectrum

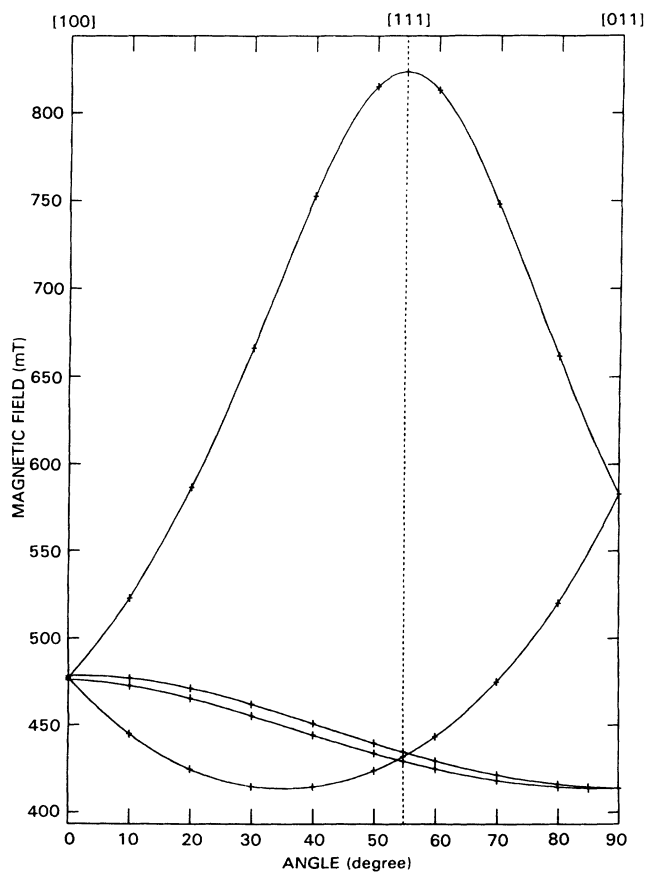


FIG. 5. Angular dependence of the EPR spectrum Si-NL44 measured at microwave frequency $\nu = 23.075$ GHz for rotation of the magnetic field in the (011) plane. Due to the small hyperfine splitting and the large anisotropy of the g value, only the center of each hyperfine spectrum is given. The solid curves are simulated ones with parameters given from the fit using spin Hamiltonian (7).

could be analyzed with the spin Hamiltonian

$$H = \mu_B \mathbf{B} \cdot \vec{g} \cdot \mathbf{S} + \mathbf{S} \cdot \vec{A} \cdot \mathbf{I}, \quad (7)$$

with $S = \frac{1}{2}$ and $I = \frac{1}{2}$. In this case the experimental points could be fitted with the maximum deviation of 1.5 mT. The results are given in Table I. The value $g_{\perp} = 3.9846$ as obtained from the analysis with spin $S = \frac{1}{2}$ indicates that the resonance is observed in the ground-state doublet of a spin quartet, with real spin $S = \frac{3}{2}$, split by a crystal field. However, since g_{\perp} is measurably smaller than $2g_{\parallel}$, the splitting between the two doublets, as induced by the trigonal crystal field, is not much larger than that caused by the magnetic field. In such a situation an analysis with an effective spin $S = \frac{3}{2}$, taking into account also spin-spin interaction, is more appropriate. The spin Hamiltonian is written as

$$H = \mu_B \mathbf{B} \cdot \vec{g} \cdot \mathbf{S} + \mathbf{S} \cdot \vec{A} \cdot \mathbf{I} + D [S_z^2 - \frac{1}{3}S(S+1)], \quad (8)$$

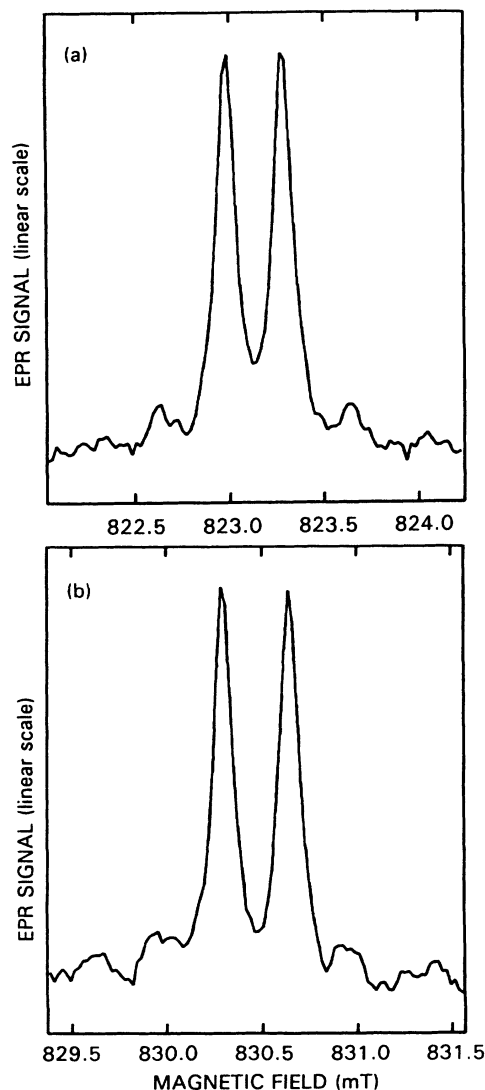


FIG. 6. EPR spectrum of the Si-NL44 center at $g_{\parallel} = 2.0028$ for $\mathbf{B} \parallel [111]$ showing the hyperfine structures due to different silver isotopes: (a) the ^{107}Ag hyperfine structure ($\nu = 23.075$ GHz); (b) the ^{109}Ag hyperfine structure ($\nu = 23.277$ GHz).

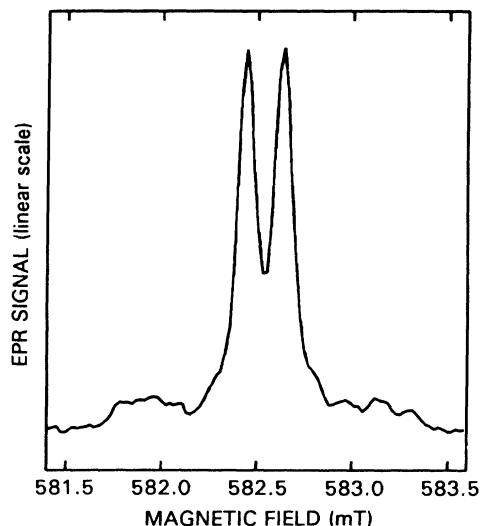


FIG. 7. EPR spectrum of the Si-NL44 center at $g = 2.8298$ for $B \parallel [011]$ showing an unresolved hyperfine interaction with an impurity that has a natural abundance of a few percent and probably a high nuclear spin.

where the D term represents the crystal-field splitting and the tensors \vec{g} and \vec{A} are constrained to trigonal symmetry along the z axis. The analysis with this spin Hamiltonian results in a fit of quality clearly superior to the previous one and gives g values in the vicinity of $g = 2$. The calculated parameters are also summarized in Table I.

The trigonal symmetry, as well as the high g value as obtained from the analysis, are again indicative of the possible relation of the Si-NL44 spectrum to a silver-impurity complex. From Fig. 6 an unresolved hyperfine interaction with an impurity of a natural abundance of a few percent can be concluded. Unfortunately, due to its low intensity and severe overlap, the hyperfine structure could not yet be disentangled. Nevertheless, as seen in

Fig. 7, in the $[011]$ direction the hyperfine structure is unusually broad and therefore suggestive of an unresolved hyperfine interaction with an impurity that has a high nuclear spin and a small nuclear moment. This observation practically rules out silicon as being responsible for the observed hyperfine splitting. The center is very similar to CrAu and CrCu pairs;^{16,21,22} however, at this stage, no further identification of the other nucleus could be made. It seems that, among the possible candidates for pairing components, chromium and titanium, which are frequent contaminants of the diffusion process, should be considered.

IV. CONCLUSION

Silver-related defects in silicon have been observed by EPR. By doping with ^{107}Ag and ^{109}Ag silver isotopes, three of these spectra, labeled Si-NL42, Si-NL43, and Si-NL44, were directly shown to be related to centers that incorporate one silver atom. Based on the electron spin, the hyperfine structure, the high symmetry, and further circumstantial evidence, the Si-NL42 spectrum is identified as the isolated interstitial silver atom Ag_i^0 .

In addition, two silver complexes have been found. The FeAg pair has been identified and the model of exchange-coupled spins is shown to account well for the observed effective spin of the center. By comparison with the similar FeAu center and in view of the electrical properties of silver, the electronic model $\text{Fe}_i^+ \text{Ag}_s^-$ is suggested for the Si-NL43 spectrum. Also, the Si-NL44 spectrum has been confirmed to be silver related. The center is very similar to CrAu and CrCu pairs and, therefore, is suggested to be identified as a pair of silver with another impurity. On the basis of the hyperfine interaction, the second impurity involved in this center could be a transition metal. For its identification, investigations of samples co-doped with silver and isotopically enriched impurities are necessary.

*Permanent address: Department of Physics, University of Hanoi, Vietnam.

†Permanent address: Institute of Physics, Ukrainian Academy of Sciences, Kiev, Ukraina.

¹F. Rollert, N. A. Stolwijk, and H. Mehrer, *J. Phys. D* **20**, 1148 (1987).

²B. I. Boltaks and Syué Shi-in, *Fiz. Tverd. Tela (Leningrad)* **2**, 2677 (1960) [*Sov. Phys. Solid State* **2**, 2383 (1961)].

³E. A. Nikolaeva and V. N. Lozovskii, *Fiz. Tekh. Poluprovodn.* **1**, 458 (1967) [*Sov. Phys. Semicond.* **1**, 381 (1967)].

⁴L. D. Yau and C. T. Sah, *Appl. Phys. Lett.* **21**, 157 (1972).

⁵L. M. Kapitonova, A. A. Lebedev, A. T. Mamadalimov, and Sh. Makhkamov, *Fiz. Tekh. Poluprovodn.* **9**, 1832 (1975) [*Sov. Phys. Semicond.* **9**, 1210 (1975)].

⁶P. Migliorato, C. T. Elliott, and A. W. Vere, *Solid State Commun.* **24**, 117 (1977).

⁷K. Graff and H. Pieper, in *Semiconductor Silicon 1981*, edited by H. R. Huff, R. J. Kriegler, and Y. Takeishi (Electrochemical Society, Pennington, 1981), p. 331.

⁸J. L. Benton and L. C. Kimerling, *J. Electrochem. Soc.* **129**, 2098 (1982).

⁹S. J. Pearton and A. J. Tavendale, *J. Phys. C* **17**, 6701 (1984).

¹⁰H. Lemke, *Phys. Status Solidi A* **94**, K55 (1986).

¹¹N. Baber, H. G. Grimmeiss, M. Kleverman, P. Omling, and

M. Zafar Iqbal, *J. Appl. Phys.* **62**, 2853 (1987).

¹²A. Fazzio, M. J. Caldas, and A. Zunger, *Phys. Rev. B* **32**, 934 (1985).

¹³G. D. Watkins, M. Kleverman, A. Thilderkvist, and H. G. Grimmeiss, *Phys. Rev. Lett.* **67**, 1149 (1991).

¹⁴G. H. Fuller, *J. Phys. Chem. Ref. Data* **5**, 835 (1976).

¹⁵J. R. Morton and K. F. Preston, *J. Magn. Reson.* **30**, 577 (1978).

¹⁶G. W. Ludwig and H. H. Woodbury, *Solid State Phys.* **13**, 223 (1962).

¹⁷E. G. Sieverts, S. H. Muller, C. A. J. Ammerlaan, R. L. Kleinhenz, and J. W. Corbett, *Phys. Status Solidi B* **109**, 83 (1982).

¹⁸F. Herman and S. Skillman, *Atomic Structure Calculations* (Prentice-Hall, Englewood Cliffs, NJ, 1963).

¹⁹S. Fraga, J. Karwowski, and K. M. S. Saxena, *Handbook of Atomic Data* (North-Holland, Amsterdam, 1976).

²⁰R. L. Kleinhenz, Y. H. Lee, J. W. Corbett, E. G. Sieverts, S. H. Muller, and C. A. J. Ammerlaan, *Phys. Status Solidi B* **108**, 363 (1981).

²¹H. H. Woodbury and G. W. Ludwig, *Phys. Rev.* **117**, 1287 (1960).

²²D. Rodewald, S. Severitt, H. Vollmer, and R. Labusch, *Solid State Commun.* **67**, 573 (1988).